RECENT PROGRESS IN THE LAND SURFACE PARAMETERIZATION EFFORT FOR THE NMC MEDIUM-RANGE FORECAST MODEL

H.-L. Pan, M. Kanamitsu, and B. B. Katz
National Meteorological Center
Washington, D.C., U.S.A.

1. INTRODUCTION

Since the recent studies of Walker and Rowntree (1977), Warrilow (1986), Shukla and Mintz (1982), Yeh et al. (1984) and others, it is becoming apparent that numerical weather prediction (NWP) models are very sensitive to the parameterization of the surface exchange processes at the atmosphere-land interface. The development of the daytime planetary boundary layer (PBL) is strongly dependent upon the parameterized surface sensible and latent heat fluxes. It is not surprising to find that convective precipitation over land is also sensitive to the soil-moisture/surface-evaporation parameterization. Re-evaporation of rain from leaf foliage and wetted soil is a key process for the convective precipitation farther inland from the moisture source.

While the parameterization of the sensible heat flux in most models is of the simple bulk-aerodynamic form based on the temperature difference between the soil surface and the lowest layer air, the parameterization of latent heat flux transport is complicated by the degree of wetness of the soil and the presence of plants. Most of the NWP models developed in the past utilized a simple "bucket" method pioneered by Manabe (1969). There is a bucket at each grid point and evaporation is reduced from a "potential" value by the ratio of soil water in the bucket and a field capacity value. In addition, the potential evaporation is evaluated assuming that the soil is saturated at the model calculated "skin" temperature. It has been pointed out by Dickinson (1983) that this method cannot realistically model the complex biosphere processes.

Toward improvement of the biosphere parameterization, there are some fairly complicated models (e.g. Dickinson, 1984; Sellers et al., 1986) that have been developed recently. Less complicated models such as Pan and Mahrt (1987) still require several levels of soil moisture and plant canopy. There is little doubt that we need better understanding of the atmosphere-biosphere interactions. Interactive feedback from the biosphere is probably as

important as feedbacks from deep cumulus and from the ocean. The level of complication needed to model this mechanism is, however, a decision that atmospheric modellers must make. This type of question has been asked concerning other feedback mechanisms as well. A notable example is the choice of the cumulus parameterization schemes. A point against a complex biosphere parameterization scheme is the lack of coordinated atmosphere-biosphere data to validate the many parameters in these schemes. Such experiments as the Hydrological Atmospheric Pilot Experiments (HAPEX) and the International Satellite Land-Surface Climatology Project (ISLSCP) experiments are only beginning to make such data available and should help in the development of such models in the future.

For short- and medium- range weather forecasts, the benefit of a detailed biosphere model is not immediately obvious. Surface evaporation interacts with radiation, clouds, and convection and, yet, each of these processes is currently only very crudely parameterized. At the National Meteorological Center (NMC) in the United States of America, we took the approach of a simple surface scheme at the level of complication comparable to the other parameterization schemes in the present generation of models. The Penman-Monteith method (hereafter refered to as PM) recently implemented in the medium-range forecast (MRF) model follows the above philosophy and will be described below.

2. METHOD

In the simple bucket method (Manabe, 1969) formerly used in the MRF, latent heat flux (LE) from the land surface is parameterized using bulk-aerodynamic formula :

$$LE = \beta \rho_a L C_h V (q_s(T_s) - q_a) \qquad (1)$$

where β is the soil moisture availability parameter, ρ_a is the density of air in the first model layer, L is the latent heat constant of vaporization, Ch is the turbulent exchange coefficient, V is the wind speed of air in the first model layer, $q_s(T_s)$ is the saturation mixing ratio at the surface temperature T_s (sometimes referred to as the skin temperature), and q_a is the mixing ratio

of air in the first model layer. The key assumptions of this formulation in addition to the bulk-aerodynamic exchange concept are:

1) the use of a single parameter, β, to simulate the reduction of evaporation when the soil and the vegetation are under stress, and

2) the use of saturation mixing ratio at the 'skin' temperature as the soil mixing ratio.

In biosphere models of Dickinson (1984) and Sellers et al. (1986), the emphasis is on the modification of the exchange parameter to include the resistance due to plants (stomatal and canopy) and soil. The PM model, on the other hand, addresses the second assumption and makes modification based on the method developed first by Penman (1948), modified by Mahrt and Ek (1984), that has been widely applied in hydrological, forestry, as well as agricultural research. We also adopted the simple stomatal resistance formulation of Monteith (1965) to model very crudely the biosphere effects. Since the major revision has to do with the second assumption of the simple bucket model, we can upgrade the biosphere treatment in the future on top of this model with little difficulty.

We will follow the work of Mahrt and Ek (1984) and define potential evaporation as the evaporation that can be realized if the soil is completely wet given the same environmental condition, i.e. net radiative flux and ground heat flux. The key point in this definition is the existence of a different skin temperature under the saturated soil condition (see also Sud and Fennessy, 1981). By allowing the upward longwave radiative flux and the ground heat flux to depend upon the skin temperature, we can write the surface energy balance under the saturated soil condition as:

$$(1-\alpha)\ S\downarrow + L\downarrow - \sigma\, T'^{4}_{s} = G + H(T'_s) + LE_p\ (T'_s) \qquad (2)$$

where the terms on the left-hand-side are, respectively, the net shortwave radiative flux (α is the albedo), the downward longwave radiative flux, and the upward longwave radiative flux (σ is the Boltzmann constant). The terms on the right-hand-side of the equation are the ground heat flux, the sensible

heat flux, and the latent heat flux. In contrast, the actual surface energy balance is defined as follows:

$$(1-\alpha\ S\downarrow + L\downarrow - \sigma\ T_s'^4 = G\ 1\ H(T_s) + \beta\ LE_p\ (T_s') \qquad (3)$$

where the last term is obtained from Eq. 2. The difference in the skin temperature, $T_s - T_s'$, can be larger than 10 K when the soil is dry. Using the simple bucket method, we ignore this difference by using T_s to calculate E_p and thus tend to overestimate the latent heat flux. As a result, there is strong moistening in the lowest model layers during the first 12-24 hours of forecast. At the same time, temperature in the lower layers of the model also tend to be lower during the daytime. This leads to an unrealistic Bowen ratio (the ratio of the sensible and the latent heat fluxes) even over regions of fairly wet forest land (e.g. the Amazon region). We interpret the latter as an additional problem of not parameterizing the presence of vegetation.

In Eq. (2), the single unknown variable is the skin temperature T_s'. Mahrt and Ek (1984) rederived the Penman potential evaporation formula starting from (2) (neglecting the effect of skin temperature on the upward longwave radiative flux and the ground heat flux as done by Penman, 1948) to obtain

$$LE_p = ((R_{net} - G)\ \Delta + LE_A)\ /\ (1+\Delta) \qquad (4)$$

where R_{net} is the net radiative fluxes,

$$LE_A = \rho_a\ L\ C_h\ V\ (g_s(T_a) - q_a)$$

and

$$\Delta = \frac{L}{C_p} \frac{d\ g_s}{d\ T} \Big|_{T_a} .$$

Troen and Mahrt (1986) included the effect of the lower skin temperature in R_{net} to obtain

$$LE_p = \frac{((1-\alpha)\ S\downarrow + L\downarrow - \sigma T_a^4 - G)\ \Delta + (1+\gamma)\ LE_A}{\Delta + 1 + \gamma} \qquad (5)$$

where $\gamma = (4\ \sigma\ T_a^3)\ /(\rho_a C_p C_h)$

To derive (4), the linearized form for $q_s(T_s')$:

$$q_s\ (T_s') \simeq q_s\ (T_a) + \frac{d\ q_s}{d\ T}\Big|_{T_a}\ (T_s' - T_a)$$

is used. To derive (5), the linearized form for $\sigma\ T_s'^4$:

$$\sigma\ T_s'^4 \simeq \sigma T_a^4 + 4\ \sigma\ T_a^3\ (T_s' - T_a)$$

is used. It should be noted that there is a dependence of T_s in the ground heat flux. We are presently ignoring this effect as it would significantly complicate the potential evaporation formulation.

Monteith (1965) and others suggested that, in the presence of plants, the stomatal resistance (rs) must be included and a potential evapotranspiration rate should be used in place of the potential evaporation rate. The unusually small predicted Bowen ratio over tropical rain forest regions suggests that we should include this effect. The resulting potential evapotranspiration rate when we apply the additional stomatal resistance to the latent heat flux in (2) is shown below:

$$L\ E_p = \frac{((1-\alpha)\ S\downarrow + L\downarrow - \sigma T_a^4 - G)\ \Delta + (1+\gamma)\ LE_A}{\Delta + (1+\gamma)\ (1+C_h V/\gamma_s)} \qquad (6)$$

Finally, the latent heat flux is now defined using the bucket concept as:

$$L\ E = \beta\ L\ E_p \qquad (7)$$

3. RESULTS

In Fig. 1 we present the 100 kPa relative humidity field over North America at the end of a 24-hour forecast using the operational global spectral model (Sela, 1980) of NMC. The present version of the model has a horizontal resolution of T80 and the E-physics package (Miyakoda and Sirutis, 1986) of the Geophical Fluid Dynamics Laboratory (GFDL) that uses the simple bucket method to estimate evaporation. The verifying analysis and the forecast error

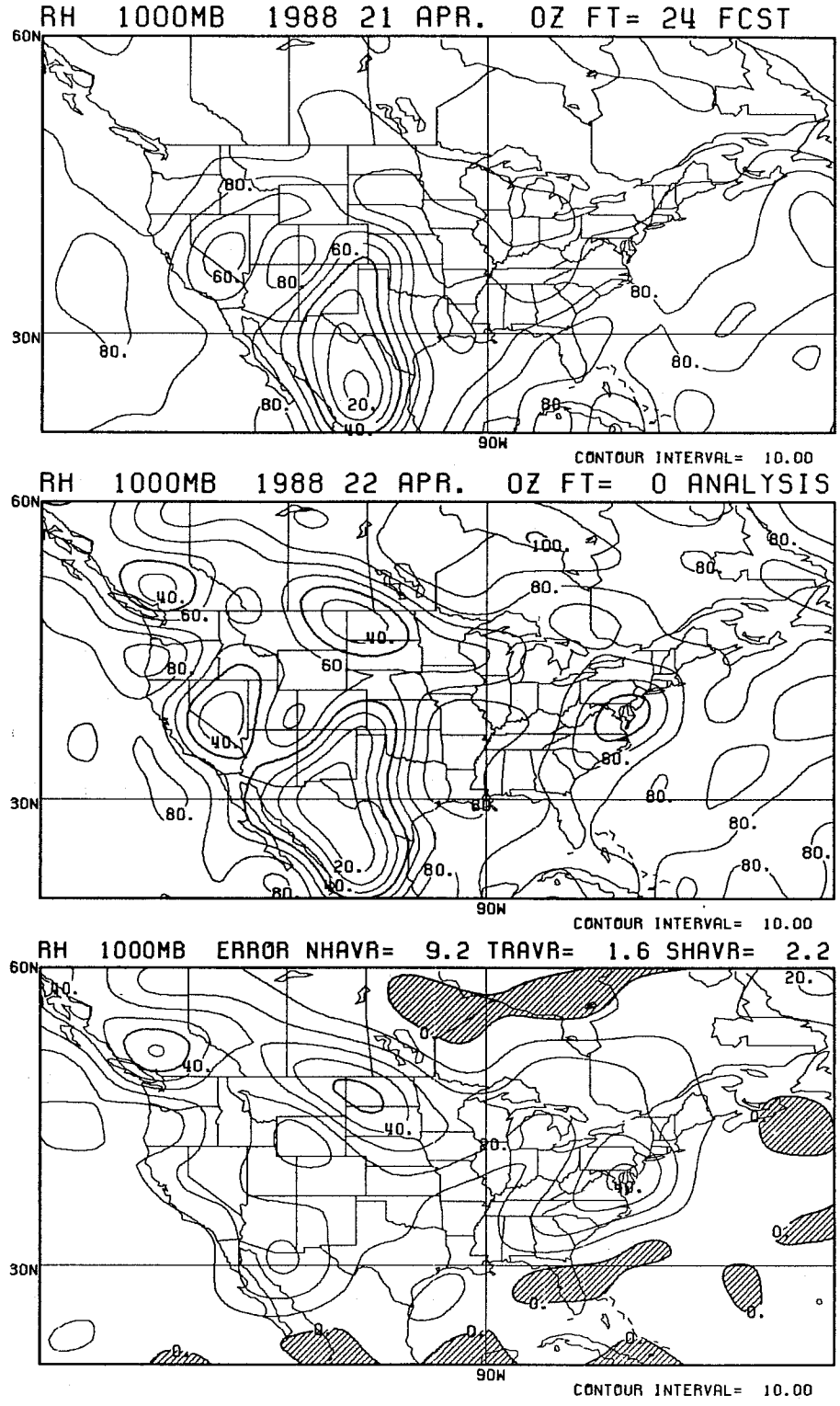

Fig. 1 a) The 24-hour forecast 100 kPa relative humidity over N America valid at 0000 GMT 22 April 1988 using the simple bucket method, b) the verifying analysis, and c) the error of the 24-hour forecast (negative errors shaded).

field are also presented (Figs. 1b and 1c). It can be seen that the forecast relative humidity exceeds 90 percent over most of the eastern U.S. and Canada. For a 0000 GMT verifying time, the local time is in the late afternoon when the observed relative humidity is usually at its diurnal minimum. It is obvious that the forecast relative humidity values are too high. Large errors are found (Fig. 1c) over most of the east coast states with a maximum error of 40 percent. The same case has been run with the PM method (Fig. 2). In addition, the data assimilation cycle was also performed using the PM method over the previous 18 hours so that an independent verifying analysis (Fig. 2b) is also available. Comparing Figs. 1a and 2a, we notice a significant decrease of the forecast values with a sharp gradient over the U.S.-Canadian border. For this time of the year (April), the model snow cover is nearly coincidental with the 90 percent relative humidity contour. Looking at the forecast error field (Fig. 2c), we see a general decrease of the error as compared to the control experiment (Fig. 1c). Even the certifying analysis is quite different (Figs. 1b and 2b).

Parallel forecasts using the PM method were run, once daily, for 15 days to evaluate the method. The averaged error fields for the 100 kPa level for Asia and Europe for the first nine days are displayed in Figs. 3-6. The reduction of error over Asia is nearly as large as that over N. America while the reduction over Europe is less significant possibly because this is a wet period over the region (relative humidity values are seen to be quite high). The error fields averaged over 15 days for N. America are shown in Figs. 7 and 8. There is significant improvement in the parallel forecast over the operational forecast in the low level relative humidity field.

For further diagnoses of the new method, we used a T40 version of the model with full diagnostics and made several experiments using the FGGE (the First GARP Global Experiment) level IIIb data. The surface energy balance for a few selected Gaussian grid points was monitored. The initial state was chosen at 0000 GMT 31 May, 1979 during the SOP II period. The components of the surface energy budget (net radiative flux, sensible heat flux, latent heat flux, and ground heat flux) are presented for a 72-hour forecast for a grid point over central U.S. for the control (Fig. 9) and the PM (Fig. 10) experiments. Also displayed are the evapotranspiration rate and the potential evapotranspiration rate for the two experiments. The change of the Bowen ratio (H/LE) from .6 to

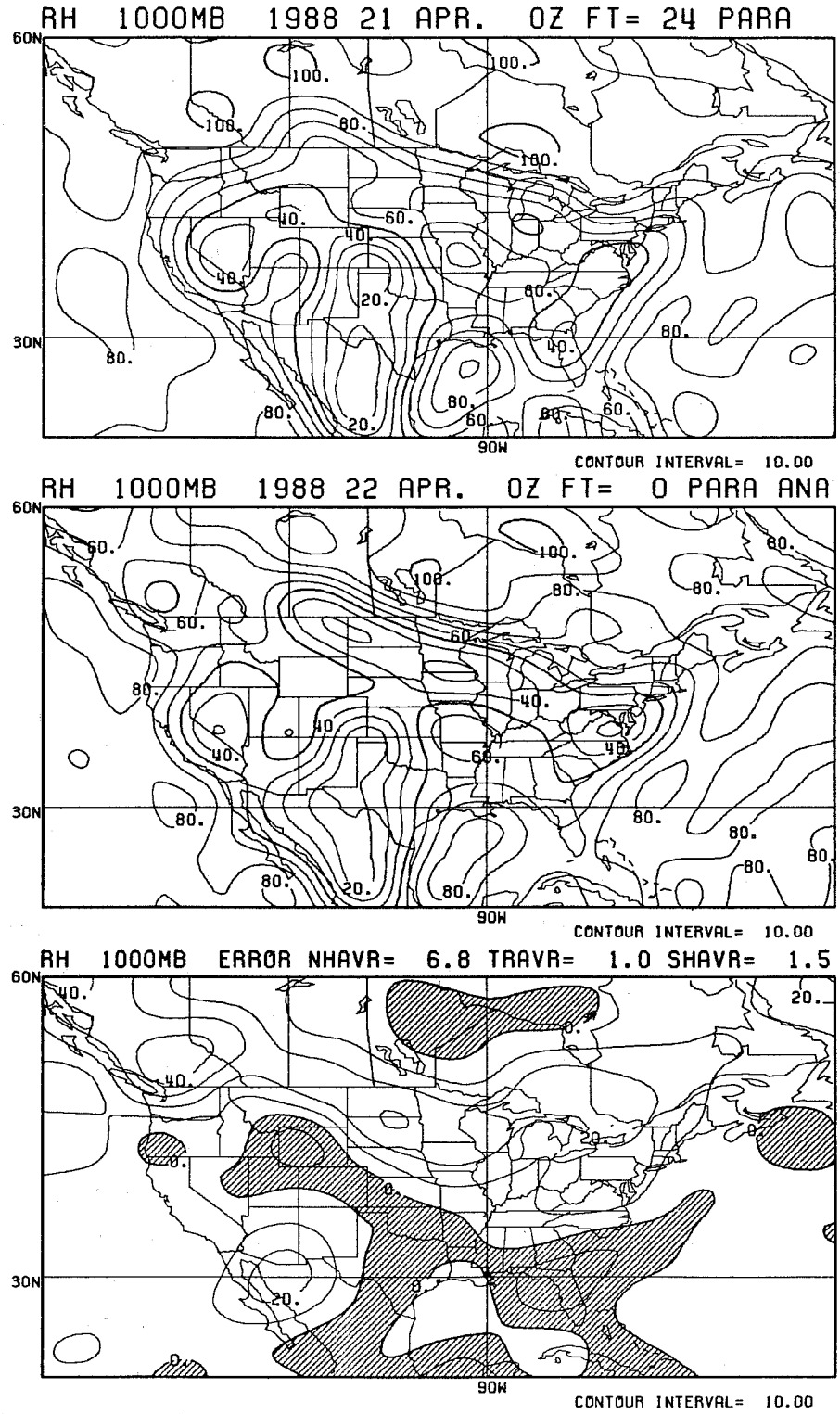

Fig. 2 same as Fig. 1 except for the Penman-Monteith method.

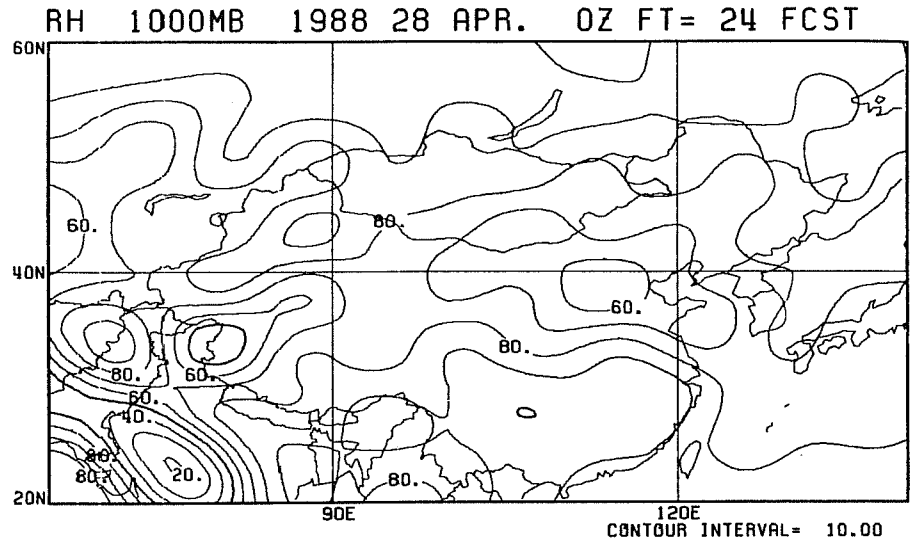

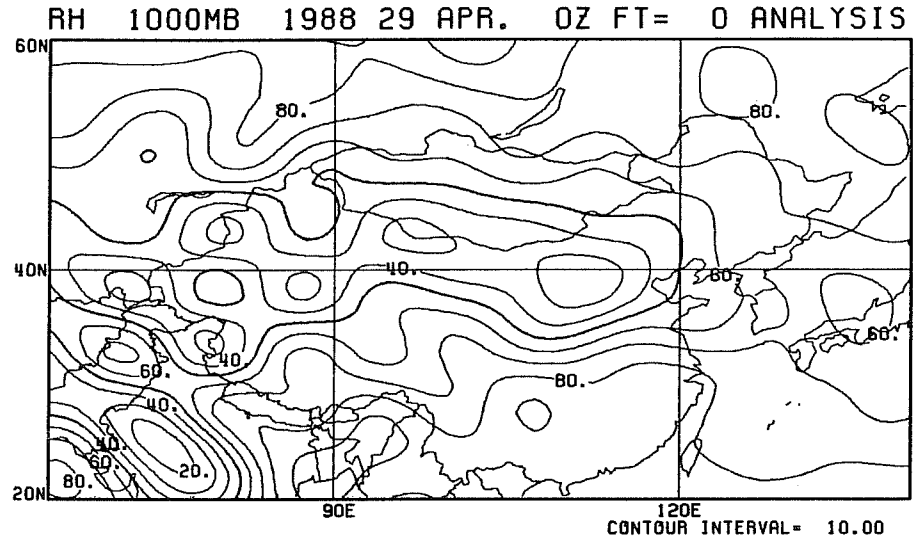

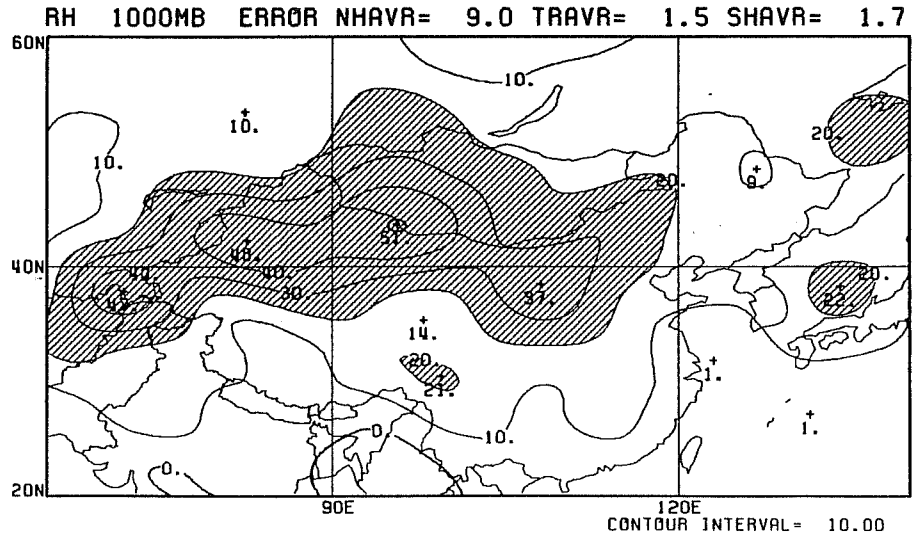

Fig. 3 same as Fig. 1 except for the average of nine cases over eastern Asia (errors greater than 20 % are shaded).

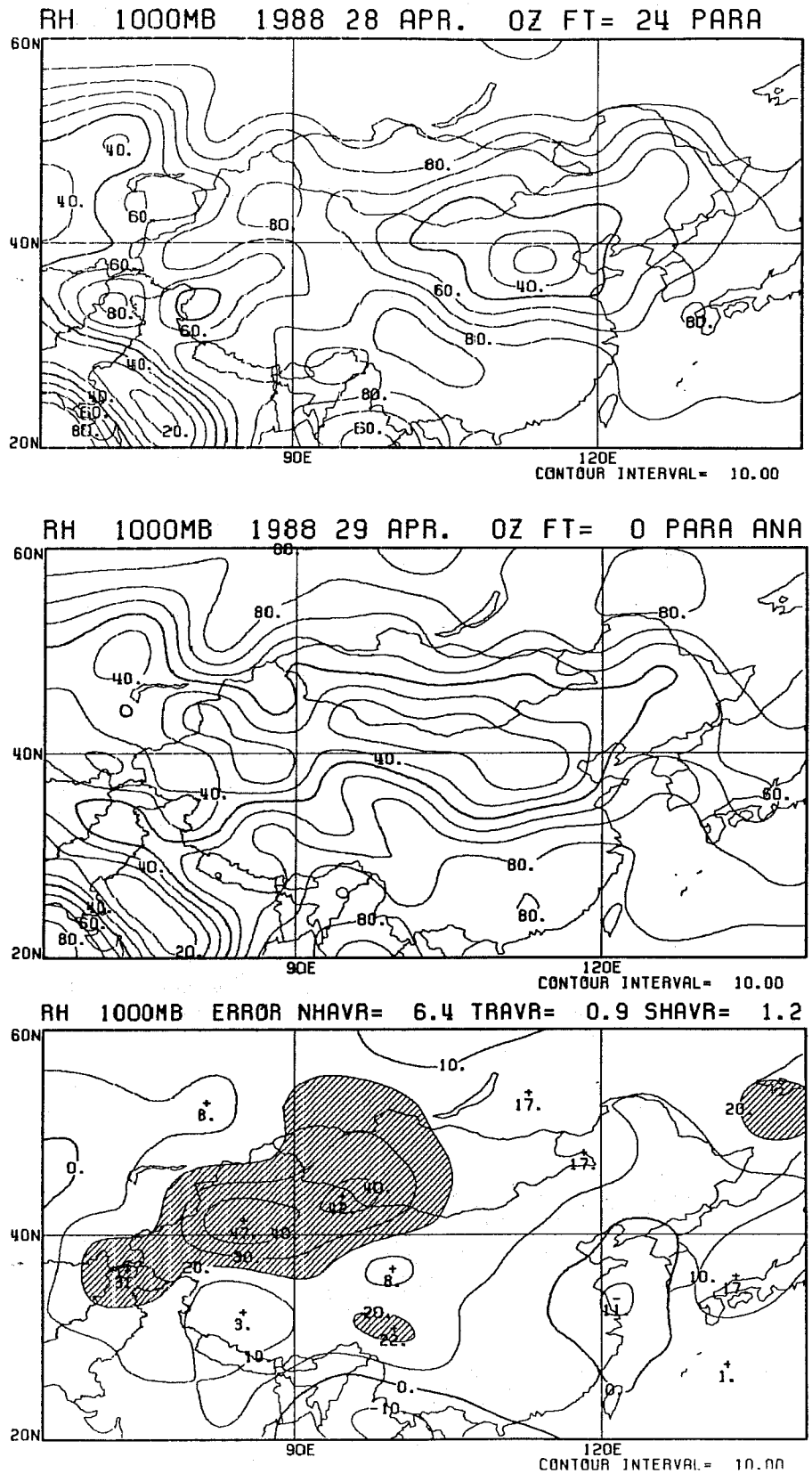

Fig. 4 same as Fig. 3 except for the Penman-Monteith method.

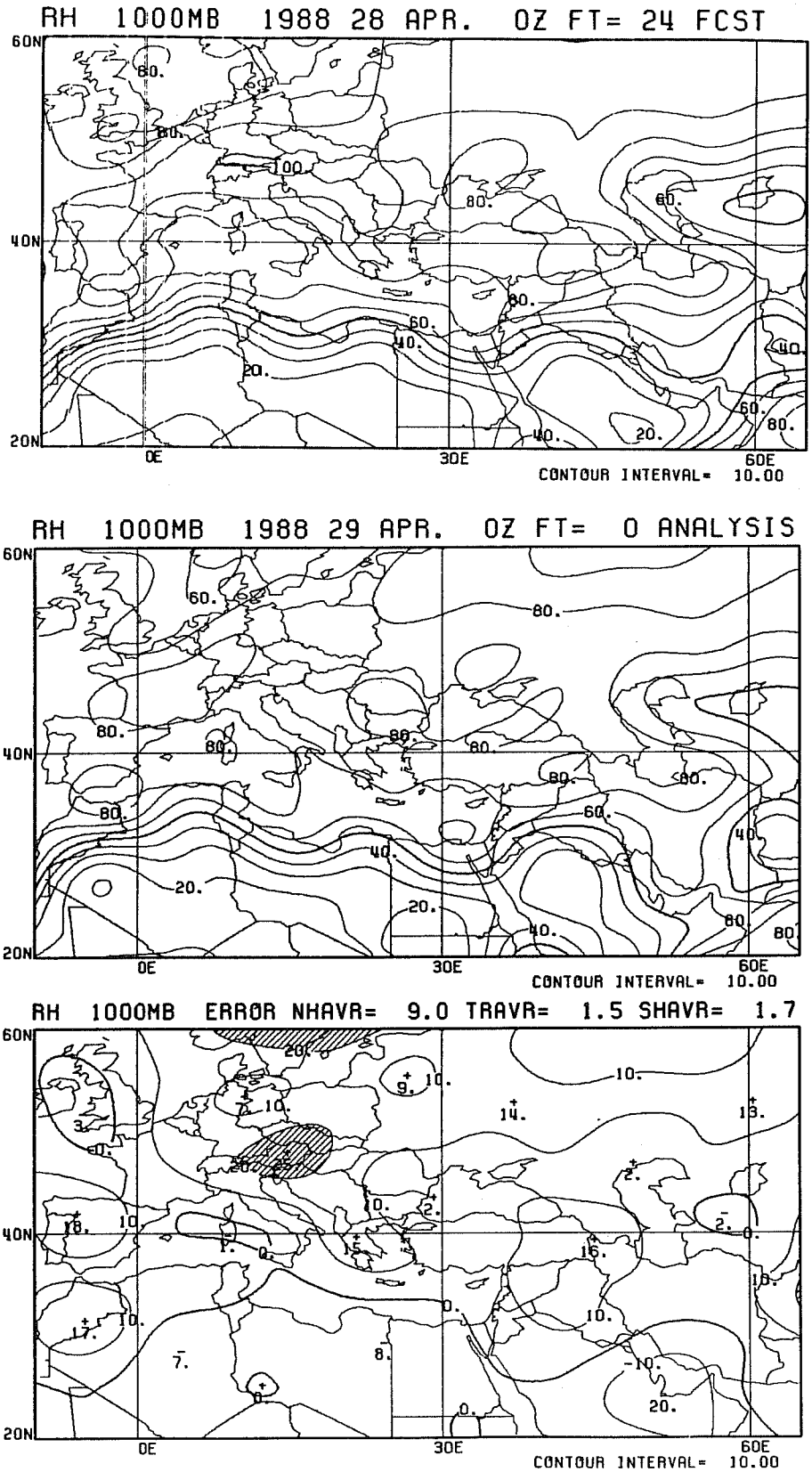

Fig. 5 same as Fig. 1 except for the average of nine cases over Europe (errors greater than 20 % are shaded).

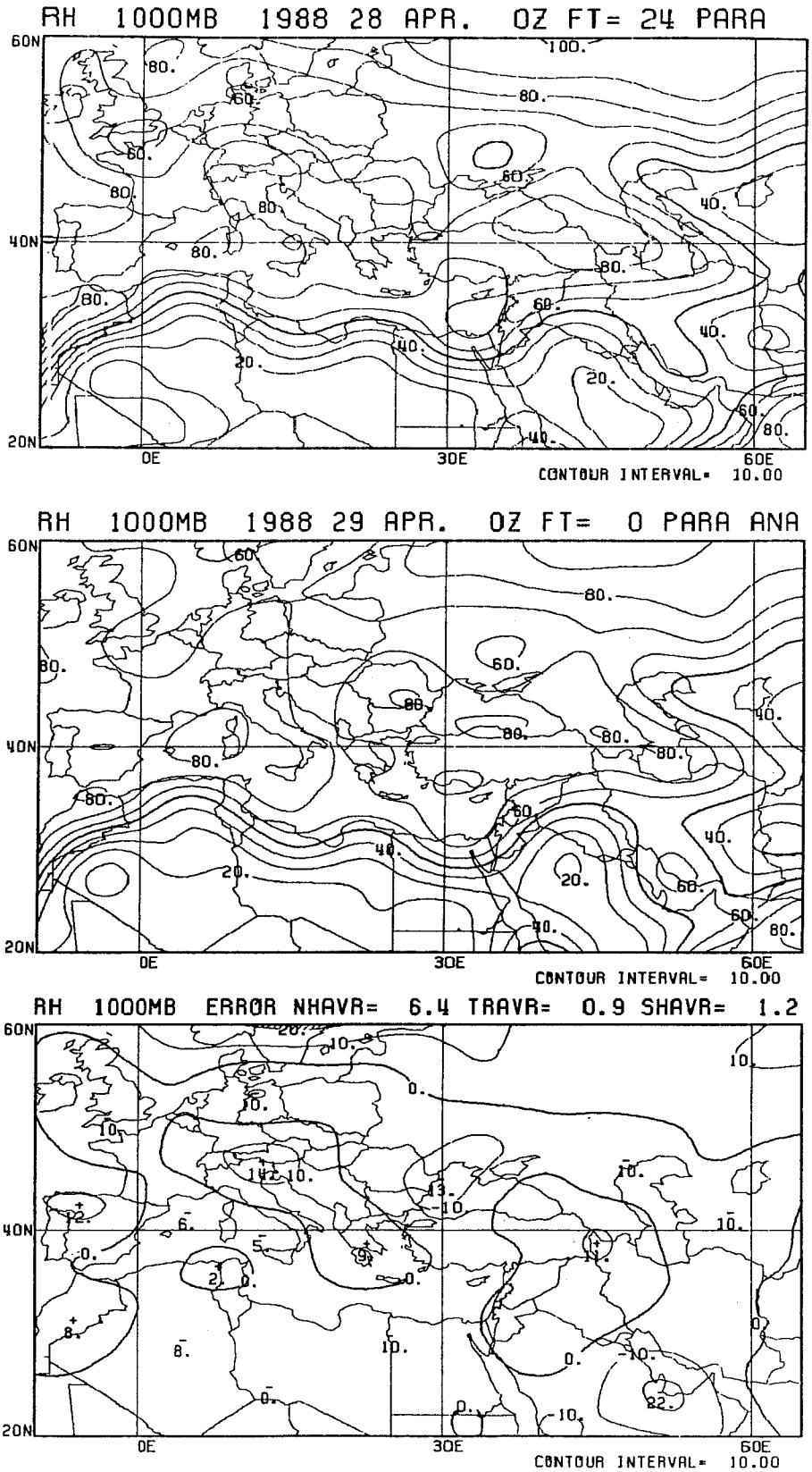

Fig. 6 same as Fig. 5 except for the Penman-Monteith method.

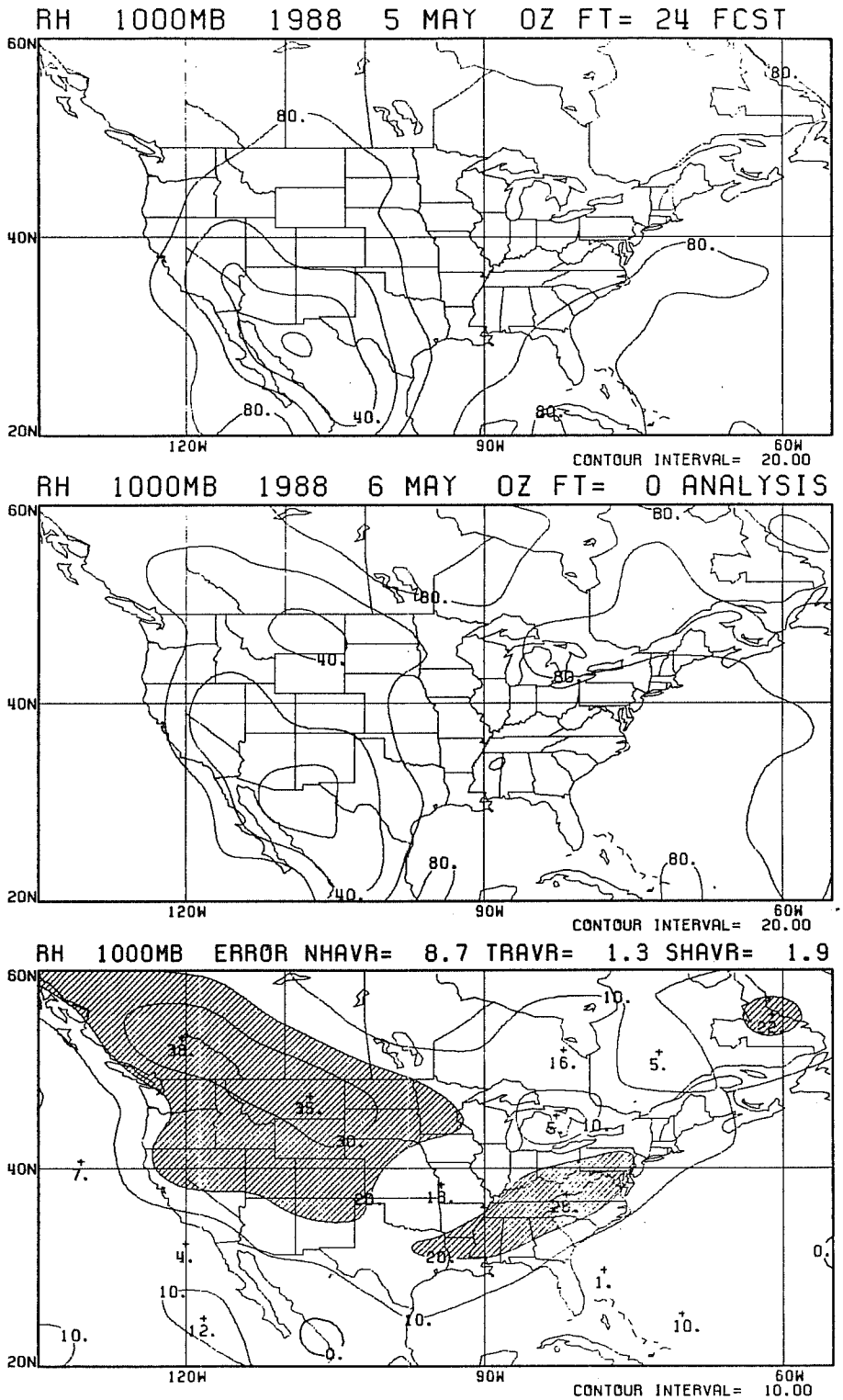

Fig. 7 same as Fig. 1 except for the average of 15 cases (errors greater than 20 % are shaded).

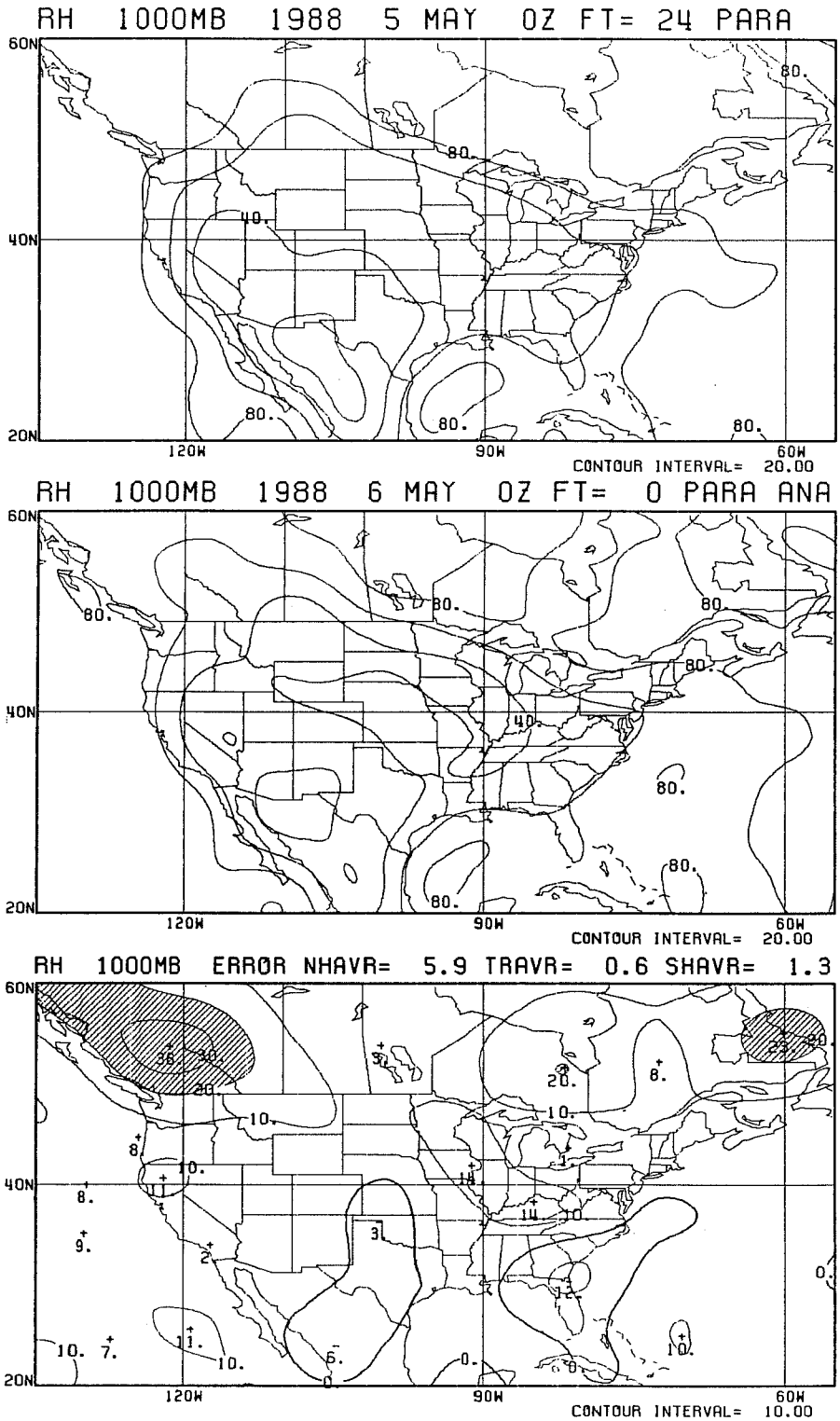

Fig. 8 same as Fig. 7 except for the Penman-Monteith method.

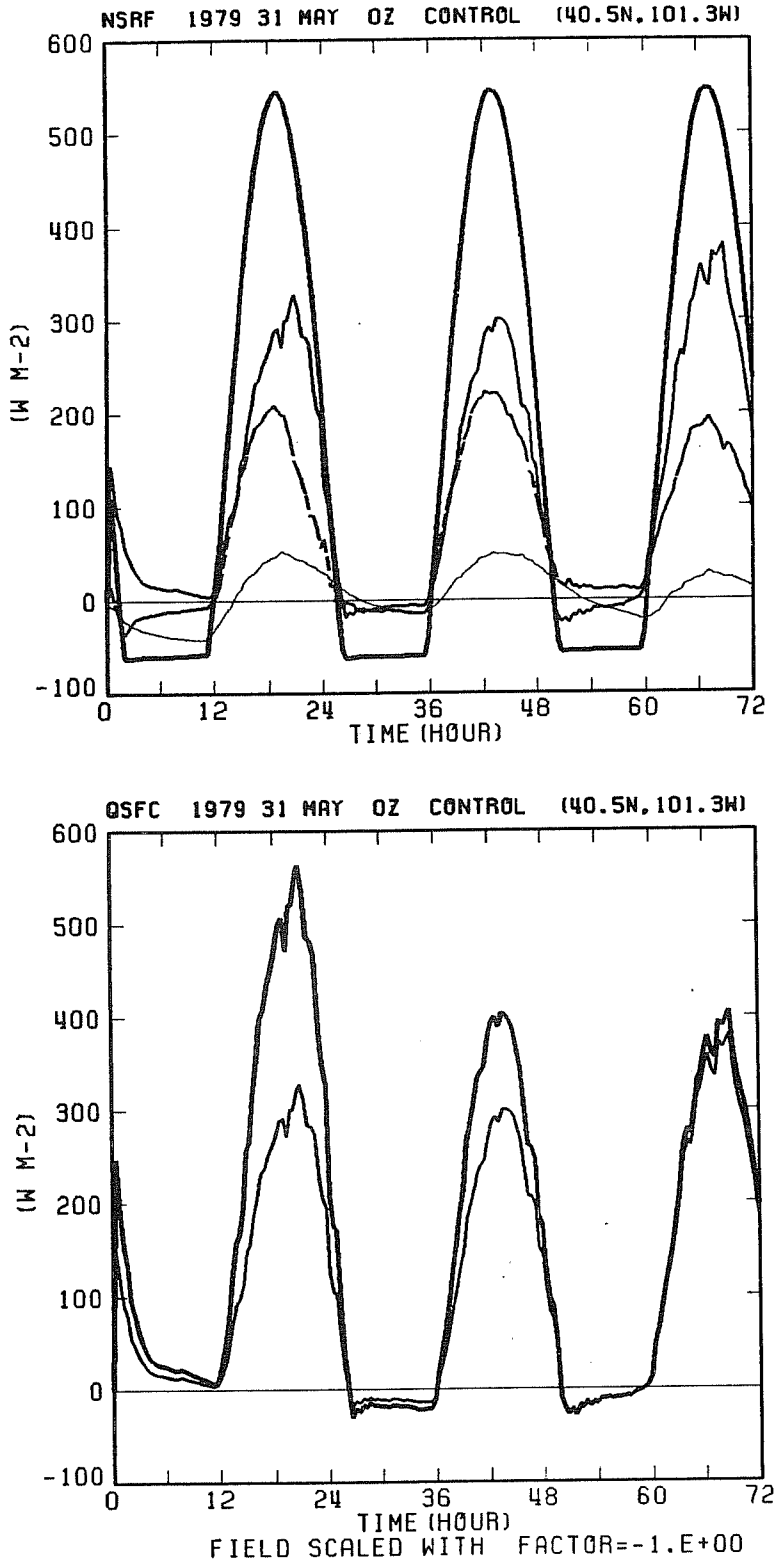

Fig. 9 a) Surface energy balance for a grid point over N. America for a 72-hour forecast using the simple bucket method (thick solid line - net radiative flux, solid line - latent heat flux, dashed line - sensible heat flux, and thin solid line - ground heat flux), and b) computed potential (thick line) and actual evapotranspiration for the same grid point.

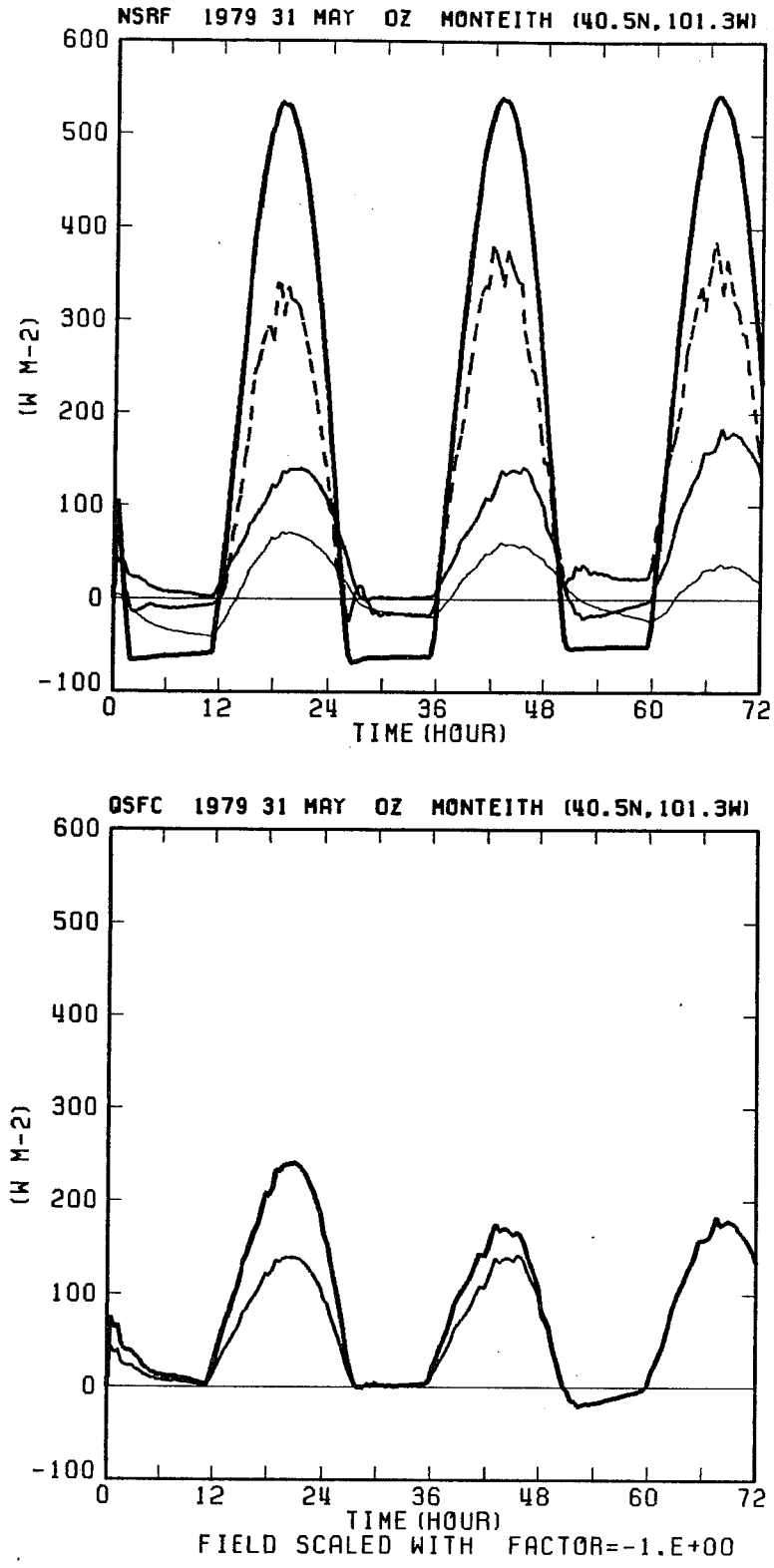

Fig. 10 same as Fig. 9 except for the Penman-Monteith method.

2.5 is a significant difference between the two methods. While the potential evapotranspiration rate for the PM method is bounded by the net radiative flux, the ground heat flux, and the relative wetness of the atmosphere, the potential rate for the simple bucket method responds primarily to the skin temperature. We note that the potential rate for the control experiment exceeds the net radiative flux on the first day and is quite close to it on succeeding days. This led to a much larger evaporation rate for the control experiment (Fig. 9) than the PM experiment even though the soil wetness parameter is nearly the same for both experiments. A similar set of graphs for a grid point in the Sahara desert region (Figs. 11 and 12) further demonstrates the strong overestimation nature of the potential evapotranspiration rate for the simple bucket method. The potential evapotranspiration rate exceeds 3000 W m^{-2} for day 1 and day 3 and is well above 2000 W m^{-2} on day 2 while the net radiative flux is only around 400 W m^{-2}.

We extended the above forecasts to 30 days to study the long term behavior of the model. In Fig. 13, we present the precipitation rate, the latent heat flux, and the sensible heat flux (converted to the same unit of mm s^{-1}) averaged over the global land surface region. For the control experiment (Fig. 13a), we see a monotonic decrease of the latent heat flux over the 30-day period with an associated increase of the sensible heat flux. For the PM experiment (Fig. 13b), the steadiness of the sensible and latent heat fluxes suggests that an equilibrium of the atmosphere-biosphere system is maintained. In Figs. 14 and 15 the same variables are presented for the northern midlatitude and the tropical regions. It can be seen that the near equilibrium characteristic of the PM method in Fig. 13 exists in both regions even though the Bowen ratio for each region is quite different.

Finally, we have recently completed an assimilation experiment where the initial soil moisture for each cycle is taken as the 6-hour forecast values from the previous cycle. The analysis-forecast assimilation cycle was repeated four times per day for a 34-day period (28 May to 30 June 1979). The evolution of the latent heat flux averaged over the global land region at 12-hour interval for the control (Fig. 16a) and the PM experiment (Fig. 16b) are seen to be quite similar to the result from the long term forecast experiments. The accompanying latent heat fluxes are shown in Fig. 17. The

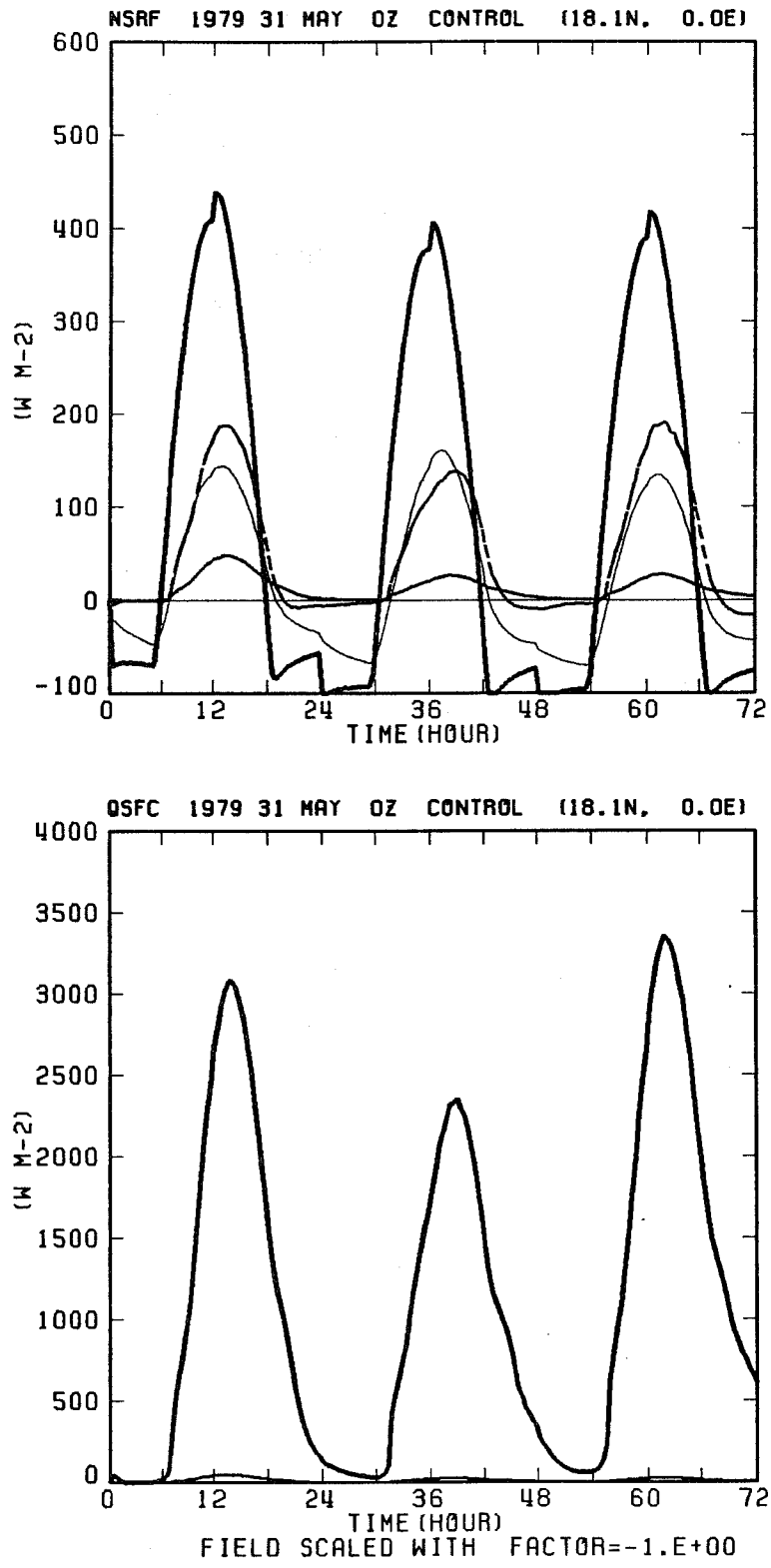

Fig. 11 same as Fig. 9 except for a grid point over the Sahara desert.

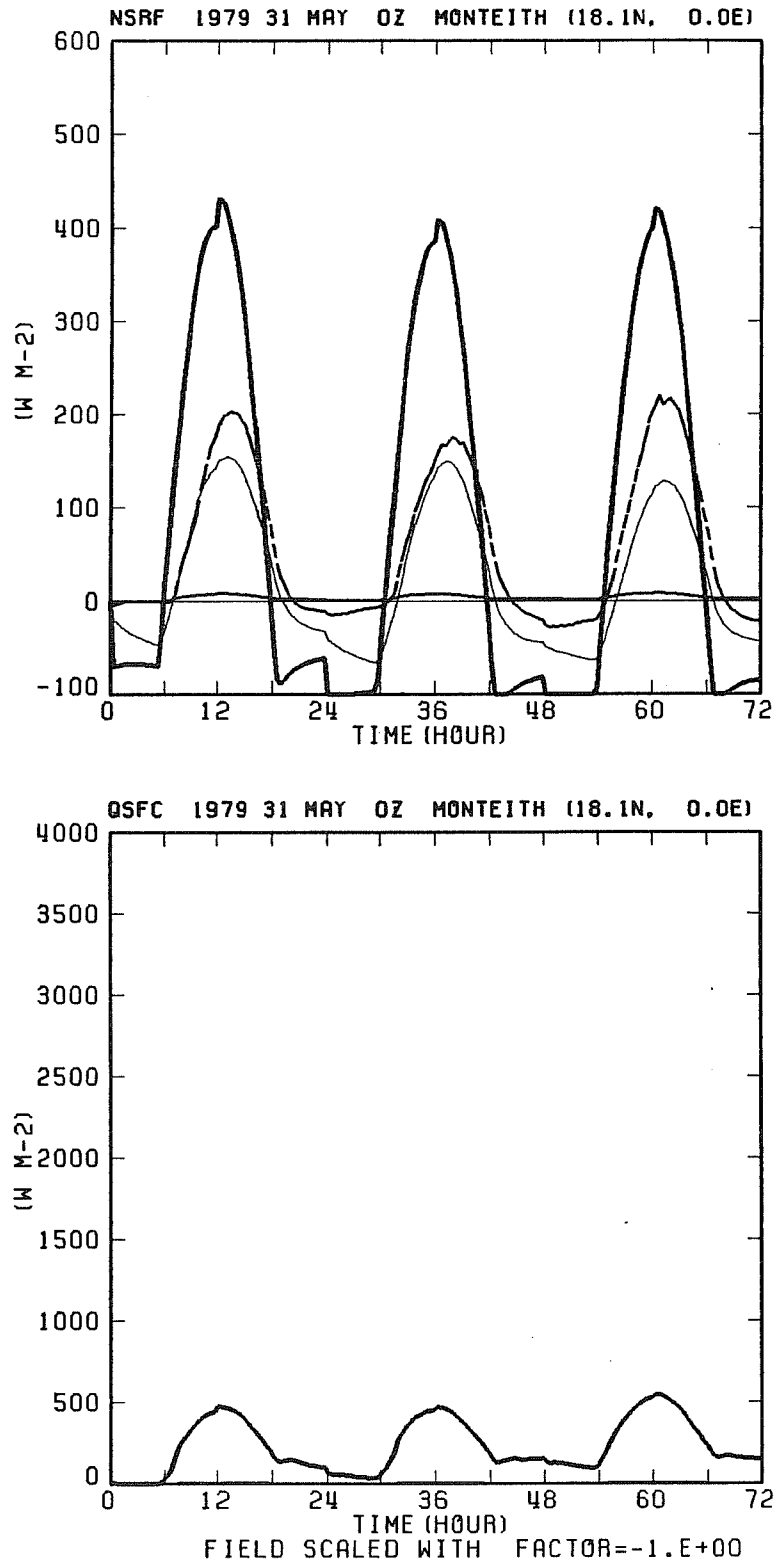

Fig. 12 same as Fig. 11 except for the Penman-Monteith method.

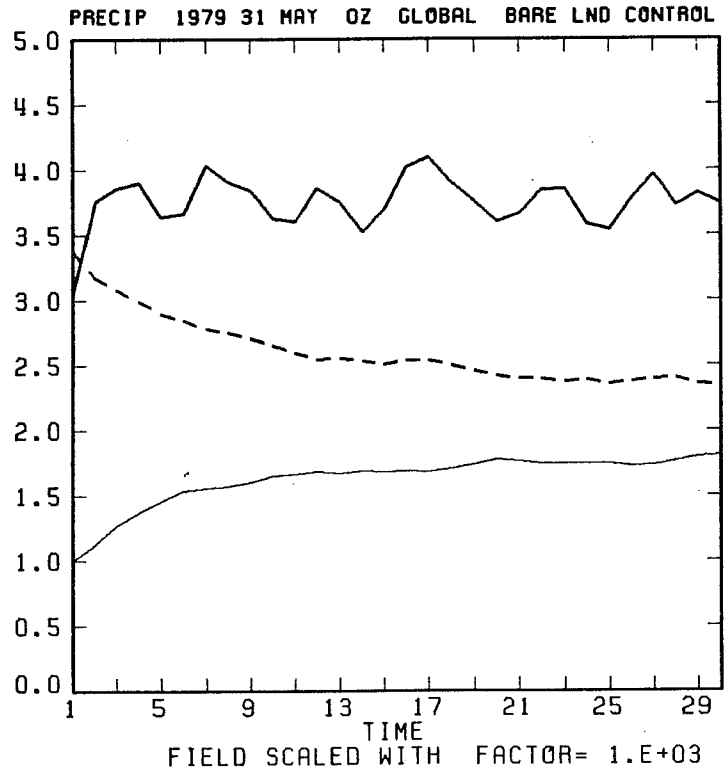

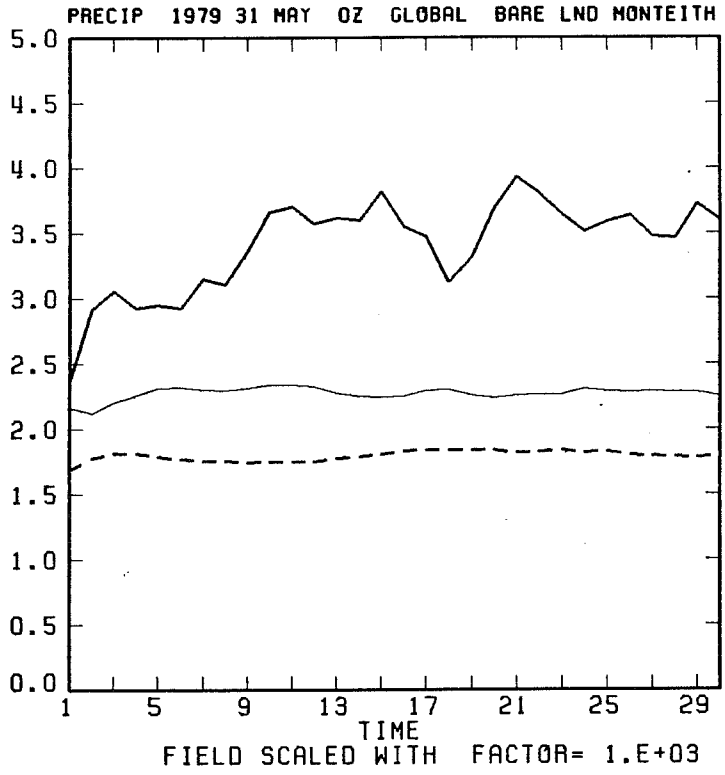

Fig. 13 Daily accumulated precipitation (thick solid line), evaporation (dashed line), and sensible heat flux (solid line) averaged over the global land area for a 30-day forecast using a) the simple bucket method, and b) the Penman-Monteith method.

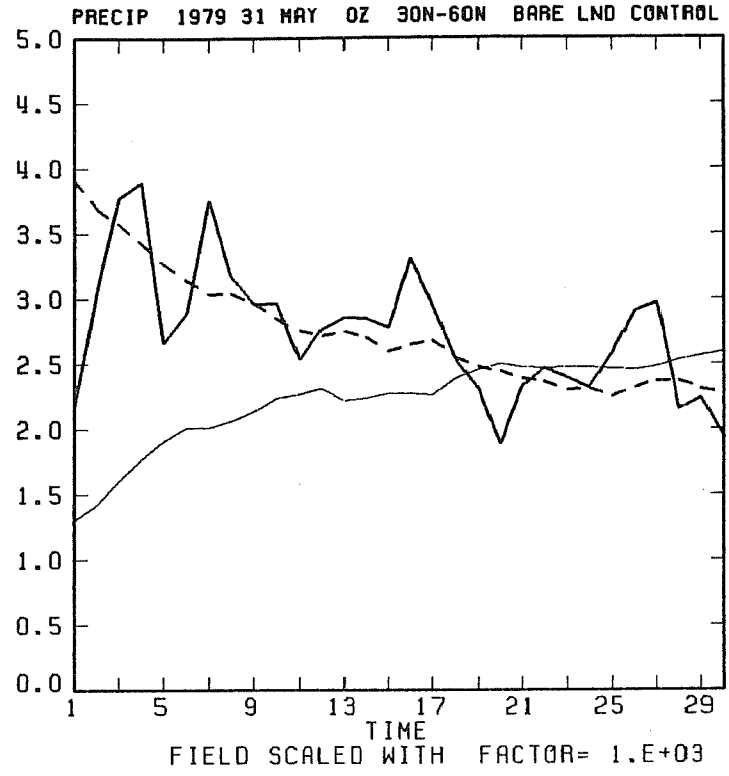

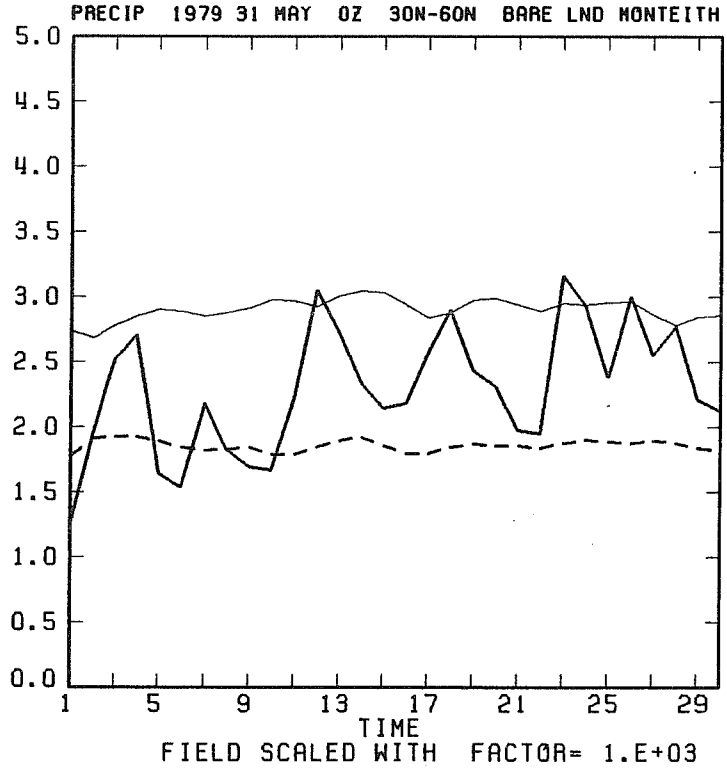

Fig. 14 same as Fig. 13 except for the average over land area between 30 N and 60 N.

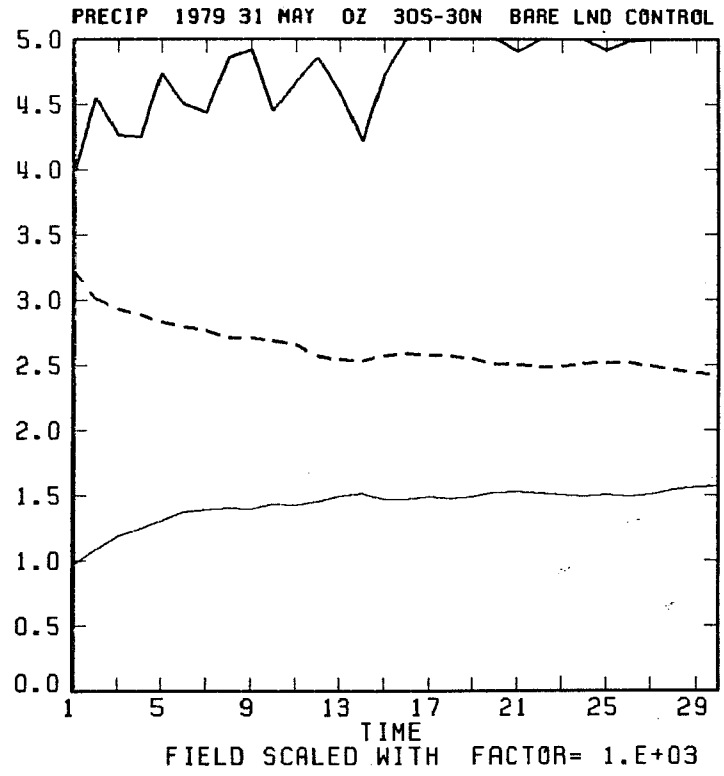

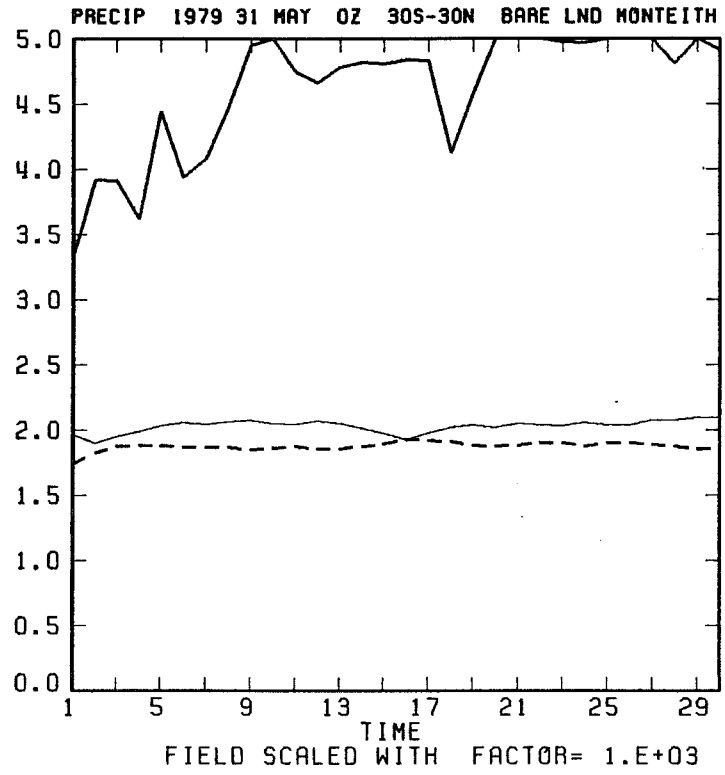

Fig. 15 same as Fig. 13 except for the average over land area between 30 S and 30 N.

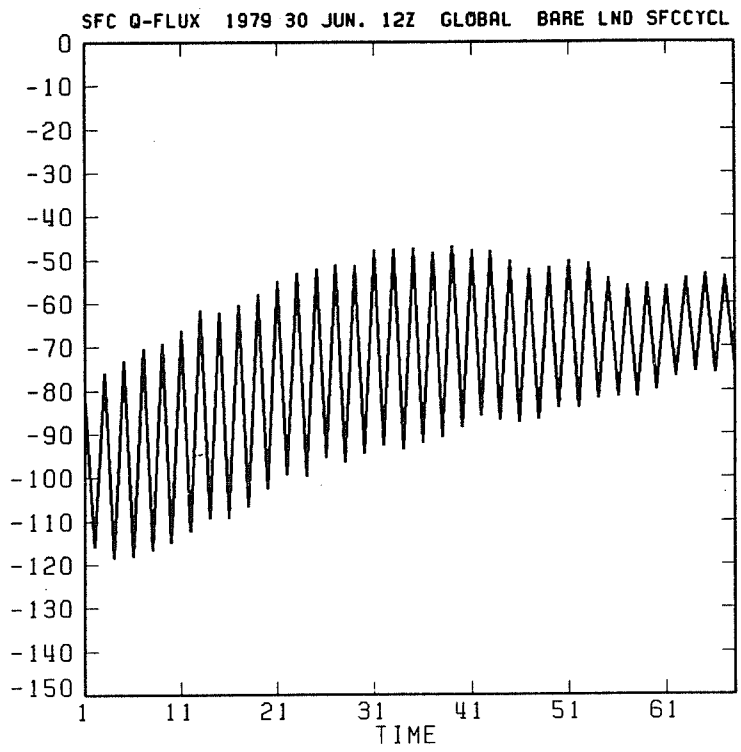

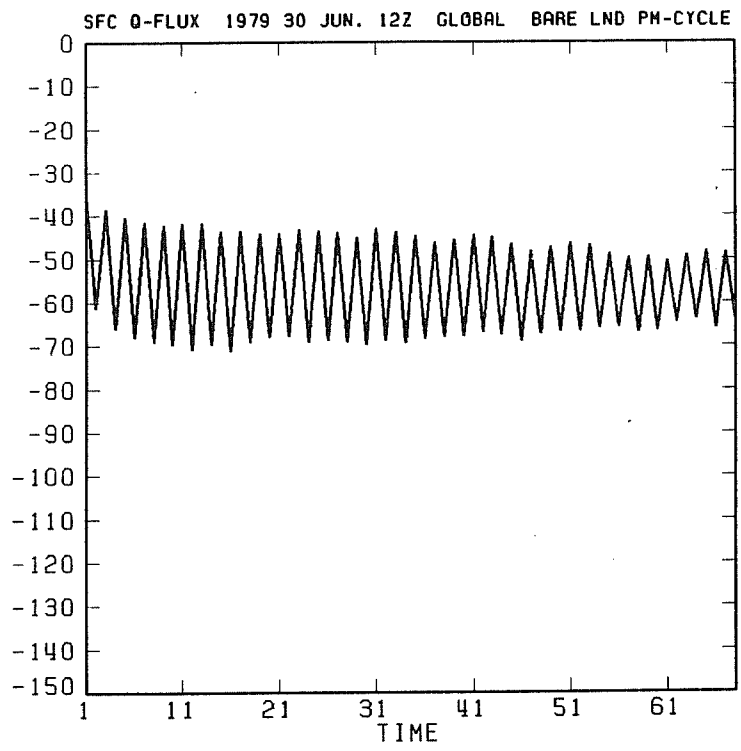

Fig. 16 Latent heat flux (positive downward) averaged over the global land area from the assimilation experiment using a) the simple bucket method, and b) the Penman-Monteith method. Fluxes are averaged over 6-hour intervals and are displayed at 12-hour intervals.

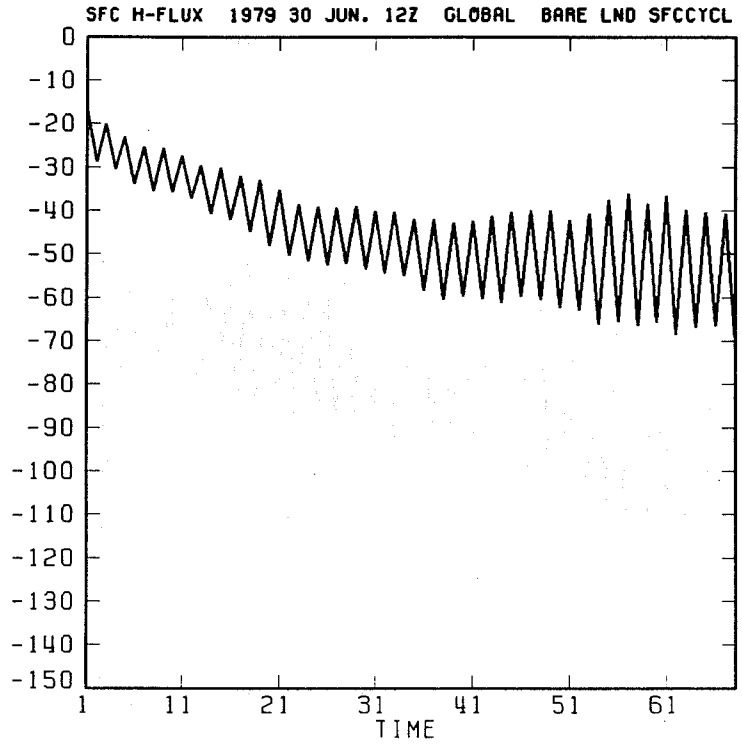

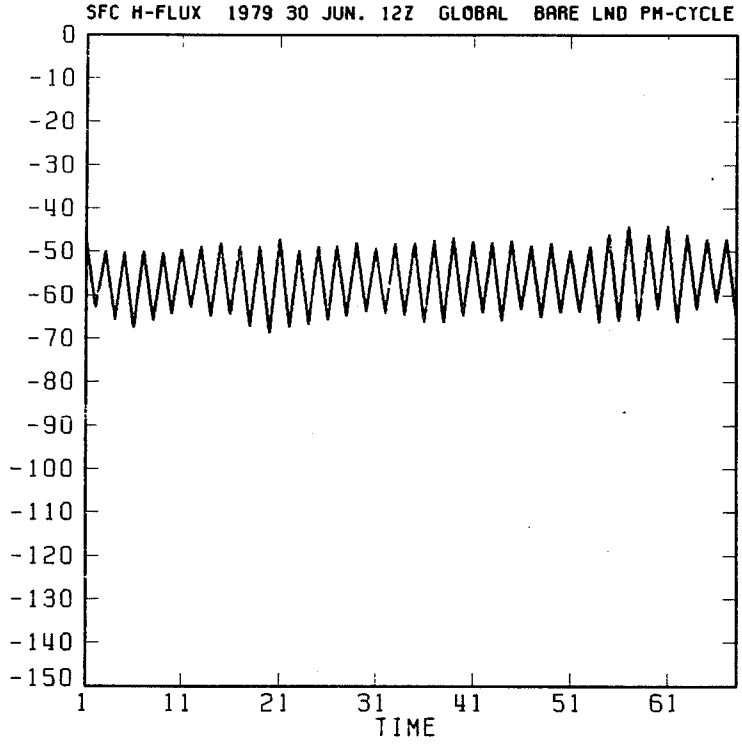

Fig. 17 same as Fig. 16 except for the sensible heat flux.

outstanding result of the experiment is the nearly constant evaporation rate for the entire period. We plan to perform a detailed diagnosis of the experiment and will report the results at a later date.

4. DISCUSSION AND CONCLUSIONS

We feel that the most important surface moisture transport mechanism over land is the evapotranspiration process from plants and we try to model this process with a bucket method that taps soil water from an implicit root zone. Over a grid area that is commonly used in the NWP models, the plant type and plant cover variations can be considerable and our uncertainty in the amount of latent heat that may be transported is sufficiently large that we feel justified at the present in using the simplest possible parameterization method. The biosphere complexities can be as overwhelming as that of clouds and radiation and require much effort to produce simple but realistic parameterization methods.

In the use of a single soil layer wetness to parameterize the stress of the soil-plant system, we are essentially modelling the evapotranspiration process only. Many important processes are completely left out. Top soil layer drying and infiltration processes are not modelled so that evaporation over desert following a rainy period would not be realistic. Canopy storage is also not modelled so that leaf wetting and drying can not be simulated. The response of the biosphere to the photosynthetically active radiation (PAR) is not explicitly considered.

Plans are underway to test more rigorously the cycling of soil wetness and soil temperature in the assimilation- prediction cycle. We are also planning to include better specification of the plant resistance using satellite derived vegetation index.

References

Dickinson, R. E., 1983: Land surface processes and climate-surface albedos and energy balance. Advances in Geophysics, 25, 305-353.

Dickinson, R.E., 1984: Modeling evapotranspiration for three-dimensional global climate models. Climate Processes and Climate Sensitivity. J.E. Hanson and T. Takahashi, Eds., American Geophysical Union, Geophysical Monograph, 29, 58-72.

Mahrt, L., and M. Ek, 1984: The influence of atmospheric stability on potential evaporation. J. Cli. Appl. Meteorol., 23, 222-234.

Manabe, S., 1969: Climate and the ocean circulation: I, The atmospheric circulatión and the hydrology of the earth's surface. Mon. Wea. Rev., 97, 739-774.

Miyakoda, K., and J. Sirutis, 1986: Manual of E-physics. Manuscript, GFDL, Princeton, New Jersey.

Monteith, J. L., 1965: Evaporation and evironment. Symp. Soc. Exp. Biol., 19, 205-235.

Pan, H. -L., and L. Mahrt, 1987: Interaction between soil hydrology and boundary-layer development. Boundary-Layer Meteorol., 38, 185-202.

Penman, H. L., 1948: Natural evaporation from open water, bare soil, and grass. Proc. Roy. Soc. A., 193, 120-195.

Sela, J. G., 1980: Spectral modeling at the National Meteorological Center. Mon. Wea. Rev., 108, 1279-1292.

Sellers, P. J., Y. Mintz, Y. C. Sud, and A. Dalcher, 1986: A simple biosphere model (SiB) for use within general circulation models. J. Atmos. Sci., 43, 505-531.

Shukla, J., and Y. Mintz, 1982: Influence of land-surface evapotranspiration on the earth's climate. Science, 215, 1498-1501.

Sud, Y. C., and M. Fennessy, 1981: A study of the influence of surface albedo on July circulation in semi-arid regions using the GLAS GCM. J. Climatology, 2, 105-125.

Troen, I., and L. Mahrt, 1986: A simple model of the atmospheric boundary layer; sensitivity to surface evaporation. Boundary-Layer Meteorol., 37, 129-148.

Walker, J., and P. R. Rowntree, 1977: The effect of soil moisture on circulation and rainfall in a tropical model. Quart. J. Roy. Meteor. Soc., 103, 29-46.

Warrilow, D. A., 1986: The sensitivity of the UK Meteorological Office atmospheric general circulation model to recent changes in the parameterization of hydrology. ISLSCP, Proceedings of an international conference. ESA SP-248, ESA, Paris, France, 143-150.

Yeh, T. -C., R. T. Wetherald, and S. Manabe, 1984: The effect of soil moisture on the short-term climate and hydrology change - A numerical experiment. Mon. Wea. Rev., 112, 474-490.